Experimental Study of Fabric Wrapped Polyurethane Shafts under Triple Point Bending

Kyle Yeomans, Liza Zamora, and Aniruddha Mitra
Undergraduate Student/Graduate Student/Faculty Mentor

Abstract

Composite materials that use fiber reinforcement can provide excellent strength to weight ratios. The objective of this experimental research is to determine which of three fiber materials, Kevlar 49, carbon fiber, or fiberglass, provides the greatest strength improvement in a standard polyurethane based epoxy sample. The high injection molding process used to produce the specimens, created a composite shaft with a core made of matrix material which is completely wrapped around a woven fiber cloth with very strong bonding between core and fibers. Two test apparatuses were designed and fabricated in the Georgia Southern University laboratory, and were used to obtain the material properties by subjecting the specimens to a three-point-bending load. Fibers separated from the core matrix due to high loads, and were followed by local buckling of the separated fibers that were under the compression region. From the experimental data, modulus of elasticity, yield strength and failure strength were estimated for all types of composites. Upon collecting, developing, and analyzing the results, it was found that the carbon fiber had the highest average modulus of elasticity, and the fiberglass produced the greatest average yield point; with Kevlar resulted in the lowest modulus of elasticity and yield point. Therefore, composites with fiber glass wrapping were found to be the strongest of the three woven fibers. Torsional and fatigue properties will be determined in future work and the effect of fiber orientations on the mechanical properties of the composites will be studied.

Keywords

Polyurethane, Kevlar, Fiberglass, Carbon-fiber

Introduction

The core base material for the fiber-composite samples selected was thermosetting polyurethane polymer. This base material was used due to high availability and low cost. The mechanical properties of the typical thermoplastic polymers are the following: lower stiffness and modulus of elasticity, a lower tensile strength, significantly lower hardness and a far greater after ductility in comparison to most metals and ceramics. The mechanical properties of thermosetting polymers are more rigid with a higher modulus of elasticity and less ductile in comparison to thermoplastics[1].

A fiber-reinforced polymer (FRP) is a composite material consisting of a base polymer-matrix composite (PMC) combined with high-strength fibers[2]. By implementing various fibers as

© American Society for Engineering Education, 2016

an external wrapping around the base polyurethane, a polyurethane based polymer-matrix composite was the resulting product. The fibers used were fiberglass, Kevlar 49 and carbon fiber. Fibers in PMCs are generally one of the following: discontinuous, continuous, or woven in a fabric form. In the case of the FRPs studied, the reinforcing fibers were in a woven fabric form with interlocking of two unidirectional fibers with the exception of the fiberglass, which was a discontinuous fiber. The two fibers selected that were woven, Kevlar 49 and carbon-fiber, were woven in what is referred to as a plain weave. This meaning that the fibers re highly interlaced, and as a result, are more resistant to shear stresses. The features and benefits that make FRPs attractive as an engineering material are their high strength-to-weight ratio and high modulus-to-weight ratios[2].

The modulus of elasticity, also known as the Young's Modulus (E), is the slope of the linear portion of the stress-strain curve for a material in the elastic region. The elastic region is defined as the portion in which no plastic deformation occurs. Hooke's Law defines the relationship in the elastic region between stress and strain[3].

$$\boldsymbol{Hooke'sLaw}: E = \frac{\sigma}{\varepsilon} = \frac{\Delta\sigma}{\Delta\varepsilon} \quad \blacksquare Equation\ 1$$

Specimen Preparation

The pressure apparatus used to create each specimen consisted of four seamless steel tubes with inner diameters of 0.5 inches. Each tube had an attachment point for a compression mold tube to be attached. A high pressure air supply line was connected to the mold tubes through a pressure regulator. The regulator air pressure was maintained between 110-120 psi during compression molding. The air supply to each mold tube could be turned on and off through a quick releasing mechanism at each attach point. Displayed in Figure 1 were the mold tubes used for the experiment. Shown in Figure 2 was the testing apparatus with the mold tubes connected to the air supply line.

(Figure 1. Mold Tubes)

© American Society for Engineering Education, 2016

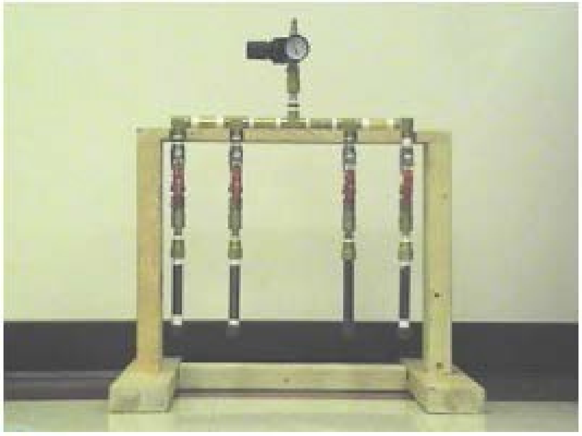

(Figure 2. Pressure Apparatus with Gauge)

The inside of the mold tubes and end caps were cleaned and sprayed with release agents before each molding process. The appropriate woven material (fiberglass, carbon fiber, or Kevlar 49) was cut into a rectangular pattern for the mold tube. Next, a piece of paper was cut slightly larger than the mat, and the mat was laid on top of the paper. The extra portions of the paper, extending approximately a quarter inch past the woven mat, were folded over to hold the mat. The two pieces were rolled up together with the paper completely encasing the mat, inserted inside the mold tube, and released so that the pieces could adjust to fit firmly inside the mold tube. Once the paper and mat were inserted inside the mold tube, the ends of the paper were torn off and the paper was pulled out of the tube leaving the mat inside the tube. Edges of the mat extended past the length of the tube; therefore, the mat was trimmed so that the edges were flushed with the ends of the tube. Next, a threaded end cap of the mold tube was screwed onto the bottom of the tube, and the tube was placed into a vise.

The ratio specified by the manufacturer of the polyurethane thermosetting polymer specified a 1:1 ratio of hardener (Part B) to resin (Part A). For each mold tube, a solution mixture was prepared by pouring 10 mL of Part A and 10 mL of Part B.

Experimental Setup of Equipment

The testing equipment consisted of a three point bending machine that was built at Georgia Southern for material research. The primary components of the machine are: the frame/sample holder, the threaded rod, the pusher/loading rod, the strain gauge, and the LVDT (linear variable differential transformer). Other components added to the apparatus include a camera with a halo light, a drill with a speed reducer (used for applying the load), and an anti- torque tab. Shown in Figure 3 was the testing apparatus with a sample in the holder.

© American Society for Engineering Education, 2016

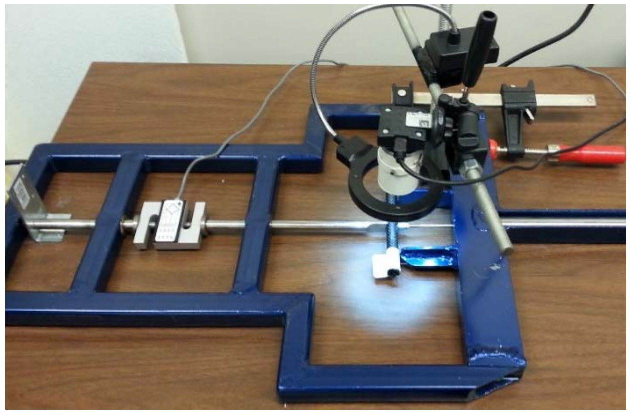

(Figure 3. Testing Apparatus)

The drill was connected to the speed reducer which allowed the loading rod to move at a constant rate. The strain gauge was located in the middle of the loading rod; this was what measured the force applied onto each specimen. The deflection inflicted upon each specimen by the applied load was measured by the linear variable differential transformer (LVDT). The camera was used to capture images of each sample throughout the loading process.

A National Instrument's Data Acquisition system was used to capture the test data. A LabVIEW Virtual Instrument program was written to process the captured data. This program consisted of two timed loops. One loop acquires data from both the strain gauge and LVDT. It then graphs the displacement and current applied force from these two sensors in real time for the operator to view. This loop also continuously writes to a file containing the displacement voltage and applied force voltage along with their corresponding times. Figure 4 provides illustration of the first loop as written in LabVIEW.

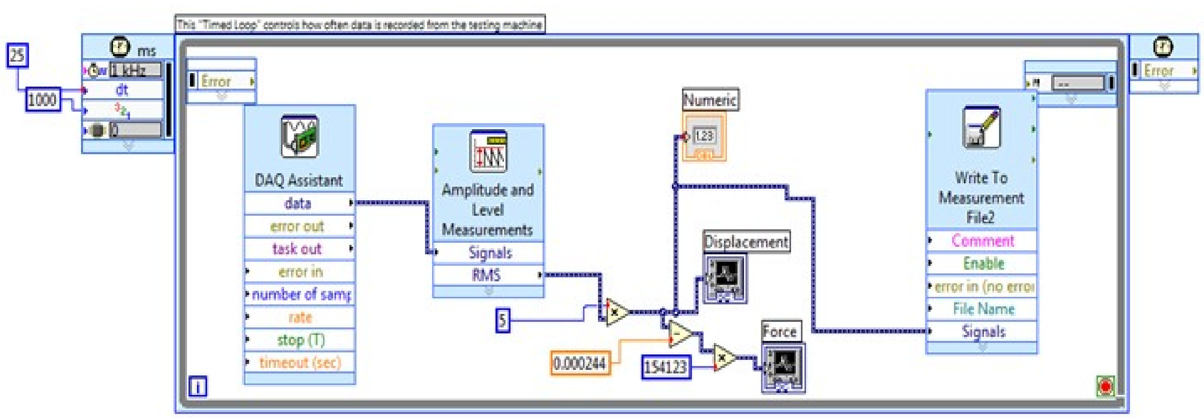

(Figure 4. Data Acquisition and Logging)

The data logged from each trial contained raw force and displacement voltages, which had to be converted into units of force and length before the data could be analyzed. This was achieved by using calibration equations for known forces and displacements on the strain gauge and LVDT rod, respectively. Once the data was converted into the proper units, the engineering stress vs. strain diagrams were generated using Excel. From these graphs, the modulus of elasticity was determined.

Testing Procedure

With the testing apparatus and computer powered on and setup for testing, a specimen was inserted between the two supports of the three point bending apparatus. The loading rod was applied to the specimen at a force of zero.

The load was gradually applied to the specimen through the drill until the specimen broke, the loading cell maxed out, or the testing apparatus reached its maximum deflection limit. Upon completion of the test, the data was exported and saved unto a Notepad (.txt) file which was then converted into an Excel (.xlsx) file. From there, the data was analyzed and processed into results.

Data and Deliverables

<u>Pure Polyurethane</u>

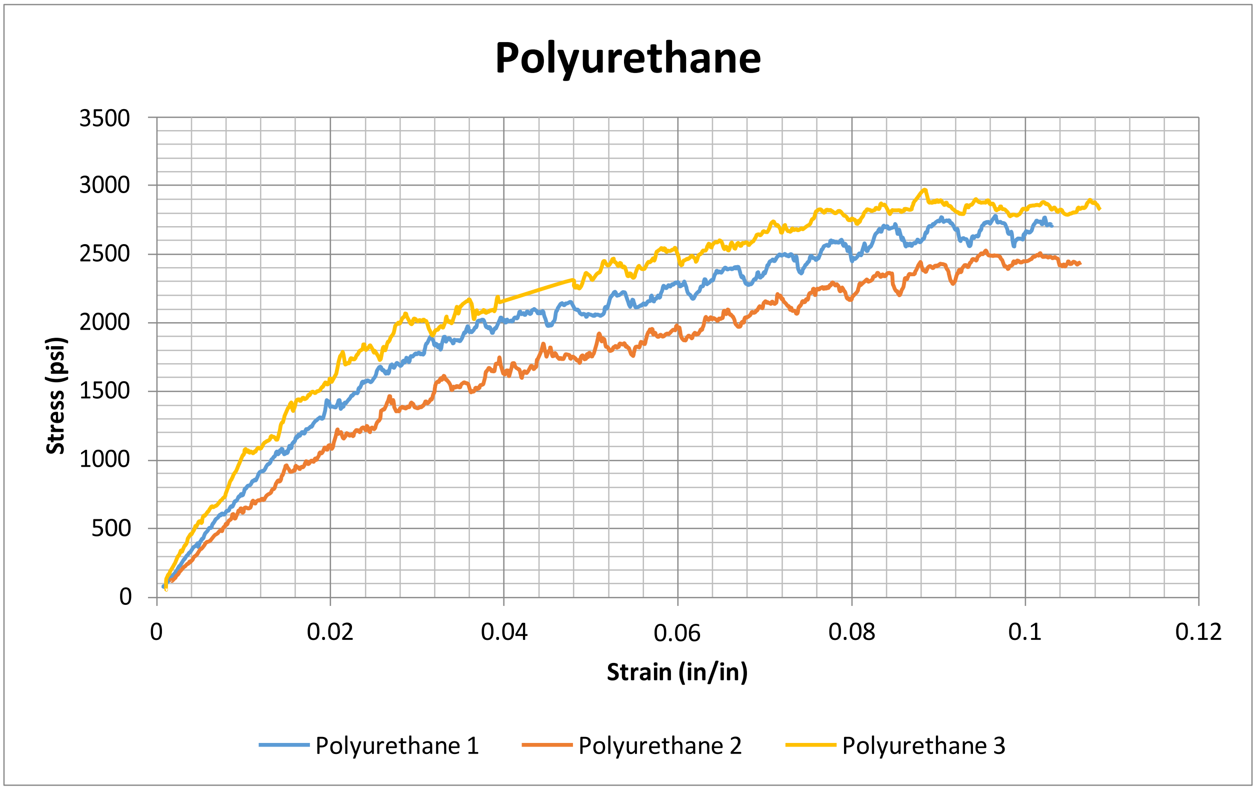

(Graph 1. Pure Polyurethane Data)

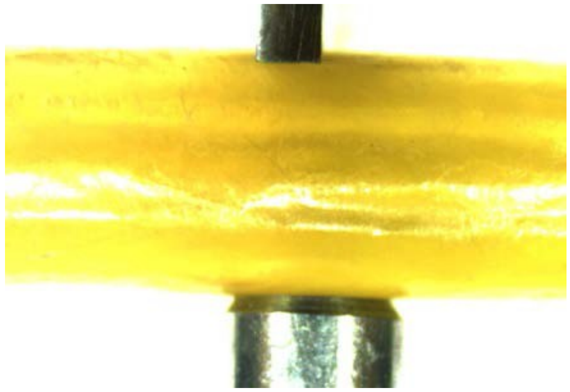

(Figure 5. Base polymer before testing)

(Figure 6. Base polymer during testing)

(Figure 7. Base polymer at end of testing)

© American Society for Engineering Education, 2016

Fiberglass

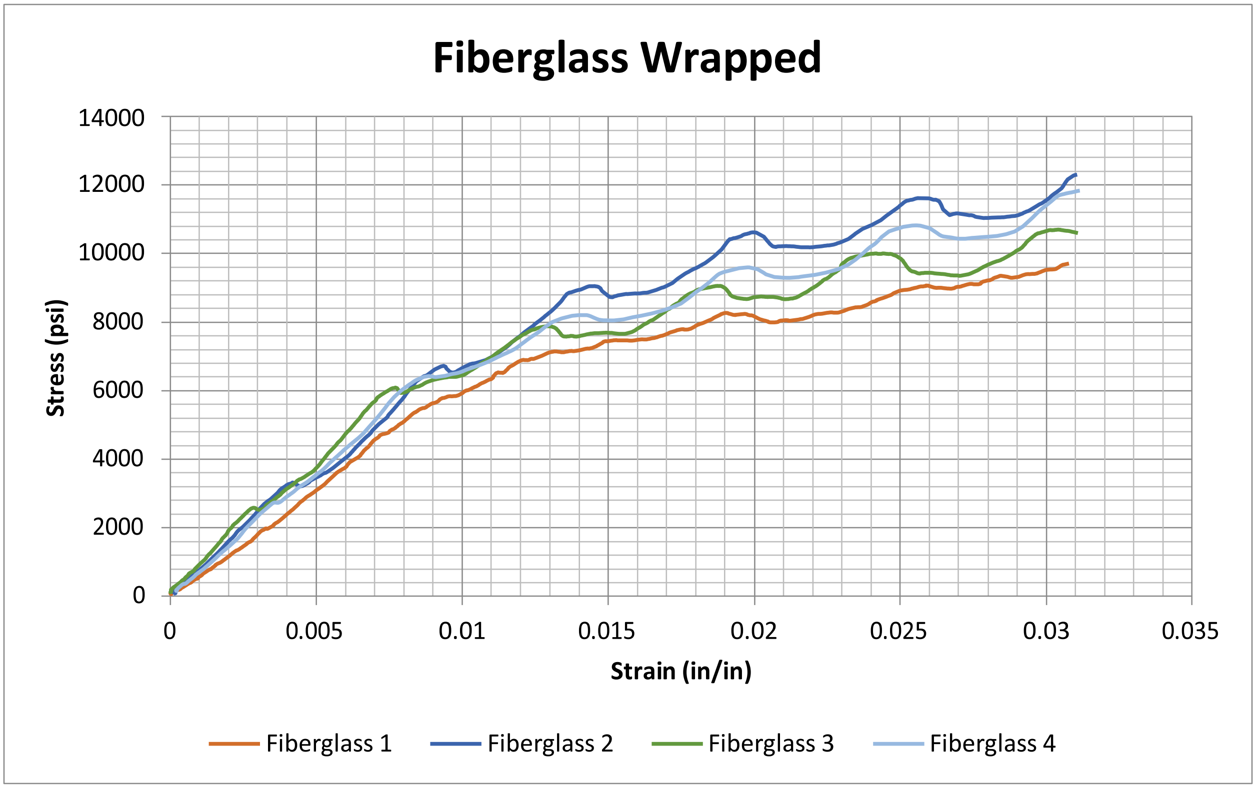

(Graph 2. Fiberglass Data)

(Figure 8. Fiberglass before testing

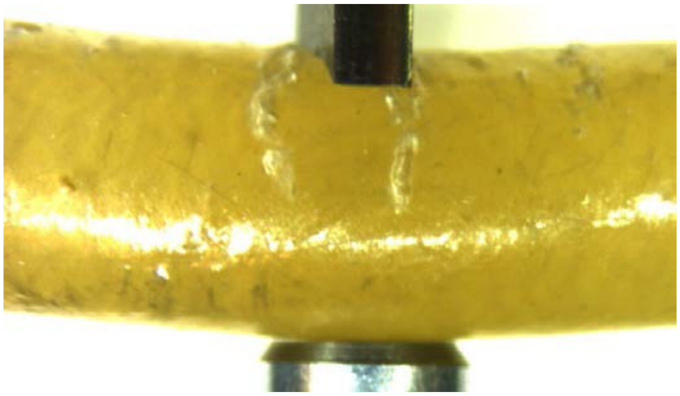

(Figure 9. Fiberglass during testing)

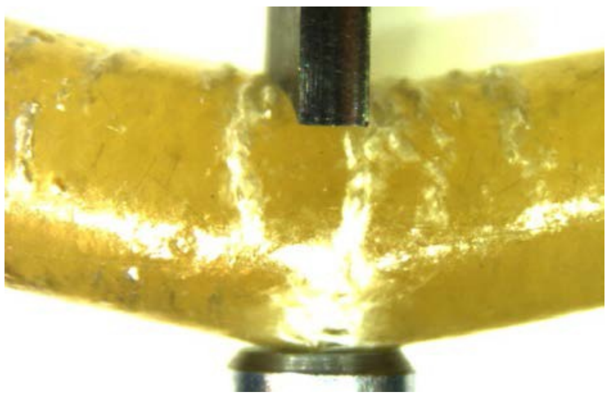

(Figure 10. Fiberglass at complete fracture)

© American Society for Engineering Education, 2016

Carbon-Fiber

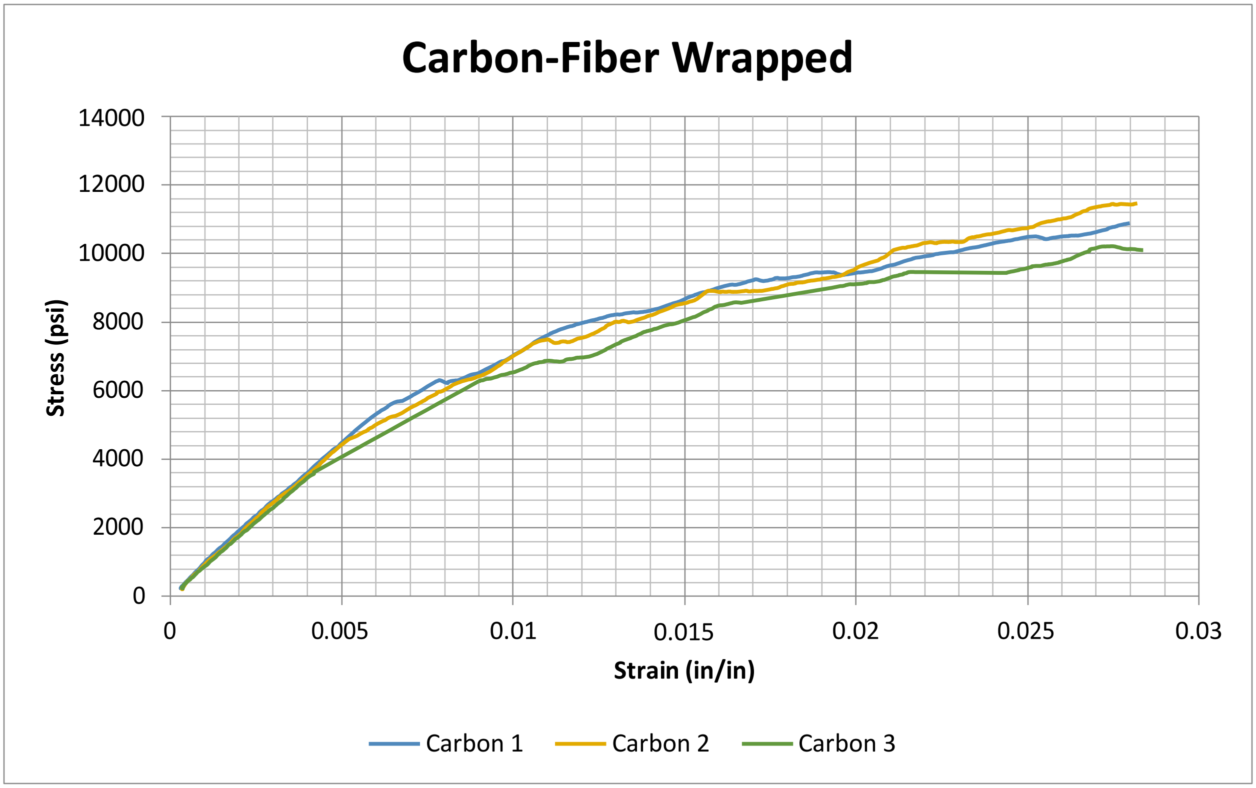

(Graph 3. Carbon FRP Data)

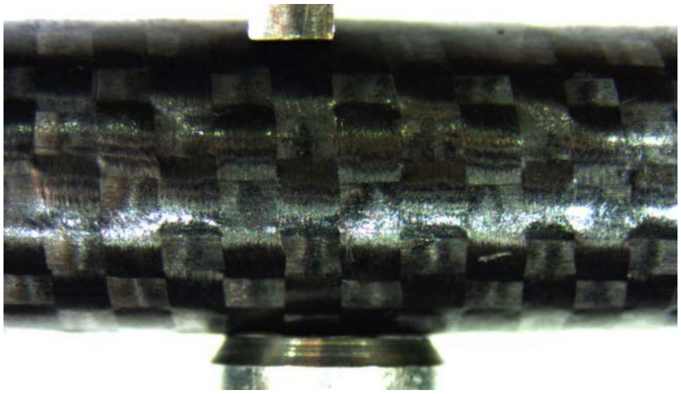

(Figure 11. Carbon-fiber before testing)

(Figure 12. Carbon-fiber during testing)

(Figure 13. Carbon-fiber at end of testing)

© American Society for Engineering Education, 2016

Kevlar

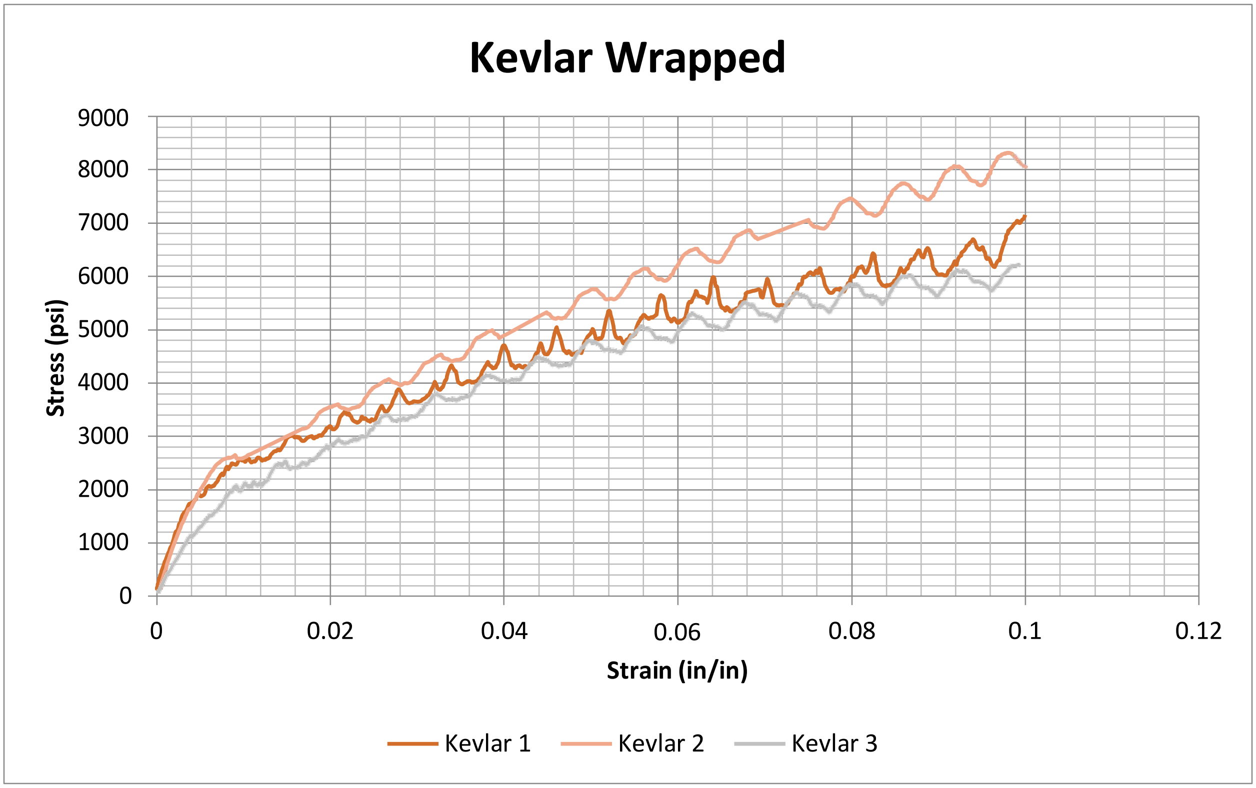

(Graph 4 Kevlar FRP Data)

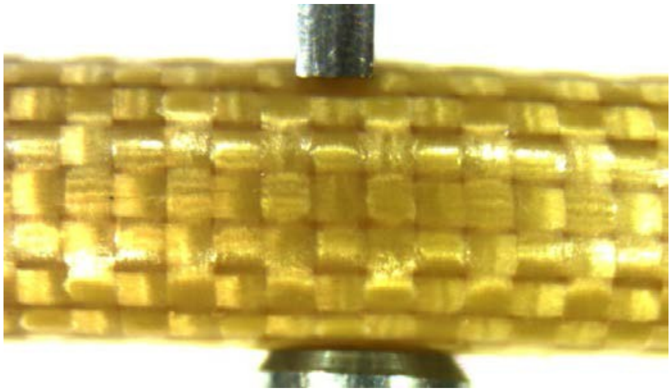

(Figure 14. Kevlar before testing)

© American Society for Engineering Education, 2016

(Figure 15. Kevlar during testing)

(Figure 16. Kevlar at end of testing)

© American Society for Engineering Education, 2016

Results

The Young's Modulus for each fiber-reinforced polymer was obtained using Equation 1. The results are tabulated into the following tables according to the specific fiber used.

Table 1

Young's Modulus for Base Polymer

Sample No.	Young's Modulus (psi)
1	69,001
2	53.851
3	79,749
Average	67,534
Std. Deviation	10,623

Table 2

Young's Modulus for Fiberglass Reinforced Polymer

Sample No.	Young's Modulus (psi)
1	545,819
2	613,332
3	567,578
4	599,401
Average	581,532
Std. Deviation	26,461

© American Society for Engineering Education, 2016

Table 3 **Young's Modulus for Carbon-Fiber Reinforced Polymer**	
Sample No.	Young's Modulus (psi)
1	847,587
2	776,708
3	822,746
Average	815,680
Std. Deviation	29,364

Table 4 **Young's Modulus for Kevlar-Fiber Reinforced Polymer**	
Sample No.	Young's Modulus (psi)
1	248,223
2	290,895
3	211,673
Average	250,263
Std. Deviation	32,374

Table 5 **Enhancement of Young's Modulus over Pure Polyurethane**	
Sample	Magnitude of Increase
Fiberglass	8.61
Carbon-Fiber	12.08
Kevlar	3.13

© American Society for Engineering Education, 2016

Observations

The observations made from the testing process and the compiled results will be presented in the following order: base polymer, carbon-fiber, fiberglass, and lastly Kevlar.

The pure polyurethane specimens exhibited continuous bending or deflection throughout the loading period. The samples continued to deflect rapidly until failure. These samples were observed to be only semi-rigid with a highly elastic behavior. The applied load was minimal with a large deflection until the specimens failed. The pure polyurethane samples never actually broke but rather, deformed to such a high extent so that the specimens slipped out of the samples; this point was concluded to be the point of failure. The fluctuations in the stress-strain diagram (as shown in Graph 1) are considered to be a result of such high formation and the resulting slips on the two supports.

The loading for the carbon-fiber samples was applied slowly and consistently with the deflection occurring at the top of the specimens. As loading was applied the fibers along the top of the specimen (those under compression) began to buckle and delaminate from the resin. Meanwhile, the fibers at the bottom (which were under tension) remained encased within the resin matrix, but eventually displayed signs of tensile strain. In time, the fibers at the bottom eventually catastrophically failed, splitting the specimens from the bottom upwards as the deflection increased at a higher rate. At the end of testing, the only fibers that remained intact were those primarily at the top of the sample that had delaminated from the resin early on. The polyurethane resin core broke cleanly and perpendicular to the length of the samples. The polyurethane core breaking failed along the path of the fiber strands that ran perpendicular to the length (the strands that were parallel to the applied loading), while minimal fibers that were perpendicular to the loading failed.

The fiberglass specimens were observed to be highly rigid and brittle in comparison, to not only the pure polyurethane samples, but also, the Kevlar and carbon-fiber. As a result, the fiberglass specimens deflected much less before total failure. Unlike the carbon-fiber or Kevlar specimens, the fibers in the fiberglass are classified as discontinuous as opposed to woven in a fabric. This resulted in no buckling or delamination of individual fibers along the top of the specimens since the fibers are dispersed within the polyurethane core. However, factures eventually began to propagate and develop along the upper section of the specimens towards to bottom. The failure of these samples was not abrupt due to the discontinuous fiber mesh in which the fibers were overlapped in all directions, allowing the load to be distributed more evenly. Nevertheless, the shafts eventually failed due to excessive tensile load at the bottom in which the core exhibited a clean break. As a result, the overall strength of these samples were highly limited in the elastic region; early on, the samples began to demonstrate plastic deformation. This is among the main factor in which the Young's Modulus is not as high as the carbon-fiber FRPs even though the fiberglass underwent a higher applied load. The fluctuations of the stress-strain graph for these samples (refer to Graph 2) were the result of the propagation and development of factures along the shaft.

© American Society for Engineering Education, 2016

As for the Kevlar 49 samples, the loading was applied at a slow, constant rate; this can be said for all FRPs as well. As loading was applied, visible buckling occurred at the top fibers on the upper half of the shaft at the section near the point of the load application. In comparison to the fiberglass or carbon-fiber, the deflection occurred more rapidly. This can be observed both graphically and from the images captured during testing. The buckling formed on the fibers at the top section, were on the fibers that ran in the longitudinal direction of the shaft. These fibers began to fold and protrude as they delaminated from the core matrix. At the bottom section of the shaft, the fibers remained smooth and attached to the polyurethane core as these fibers were under tension. When the composite shaft finally broke it was sudden and abrupt. A portion of the top fibers remained intact (approximately one third of them) while the bottom stands broke from tensile stress leaving in frayed ends of the fibers. The polyurethane core exhibited a clean, smooth failure surface. It was observed that some stand of fibers along the bottom failed before the polymer core had failed; this resembled the same failure characteristics of the fiberglass samples with its chopped, discontinuous fibers. The fluctuations of the stress-strain graph (refer to Graph 4) are assumed to be a result of the buckling in the fibers along the top section of the specimen.

Discussion

It was concluded from the results that the carbon-fiber reinforced polymer provided the greatest increase in the Young's Modulus over the base polyurethane samples. From observing the stress-strain diagram for the carbon samples (refer to Graph 3), it was noted that in order to displace the samples, it took a significantly higher load in comparison to all other samples. This phenomenon can also be cross-referenced with the screenshots taken during test, noticed in Figures 11 through 13. Comparing those to the other samples, the less displacement occurred during the carbon-fiber reinforced polymer test. The fiber with the second highest increase in the modulus of elasticity was the fiberglass, followed by the Kevlar with the lease. The fiberglass reinforced polymer was subjected to a higher loading then that of the carbon fiber, but at the same time, the strain at each corresponding stress was higher; also, the fiberglass plastic deformed more quickly than the carbon fiber. Therefore, the overall Young's Modulus of the fiberglass was less than that of the carbon-fiber.

The fluctuations in the graphs occurred for the following reasons: a result of the delamination of the fibers to the core matrix, shifting of the samples after extensive deflection had taken place, or from fracture development and propagation within the core shaft. All of the samples, including the pure polyurethane, had such fluctuations in the stress-strain curves (Graphs 1-4) as a result of one or more of these reasons. The carbon-fiber samples underwent the least amount of graphical fluctuations which is supported by the screenshots logged during test (refer to Figures 11-13). The samples with the most graphical fluctuations was that of the fiberglass; this is largely apparent in the images gathered during the testing process (see Figures 8-10) with the massive fractures that occurred parallel to the applied loading.

© American Society for Engineering Education, 2016

Conclusion

Fiber-reinforced composite materials consist of fibers of high strength and modulus embedded in or bonded to a matrix with distinct interfaces between them. The objective of the present research is to determine which of three fiber materials, Kevlar 49, carbon fiber, or fiberglass, provides the greatest strength improvement in a standard polyurethane based epoxy sample. Triple point bending tests were carried out to test these three different types of composite samples as well as the pure polyurethane samples. For the carbon-fiber, fiberglass and Kevlar reinforced polymers, the average Young's Modulus was 815,680 psi, 581,532 psi and 250,263 psi, respectively. Therefore, the carbon-fiber reinforced polymer was found to be stiffer than the polymers reinforced with fiberglass and Kevlar. The results established from the stress/strain graphs show the fiberglass having the greatest average yield point and the Kevlar reinforced polymer having the lowest.

References

1 Groover, Mikell, Fundamentals of Modern Manufacturing: Materials, Processes, and Systems 4th Edition, John Wiley & Sons Inc., Hoboken, NY, 2010, 165-166

2 Groover, Mikell, Fundamentals of Modern Manufacturing: Materials, Processes, and Systems 4th Edition, John Wiley & Sons Inc., Hoboken, NY, 2010, 199-201

3 Askeland, Donald, Pradeep, and Wendelin, The Science and Engineering of Materials 6th Edition, Global Engineering, Stamdford, CT, 2011, 211.

4 Mallick, Fiber Reinforced Composites: Materials, Manufacturing and Design 3rd Edition, CRC Press, Boca Raton, FL, 2007, 1.

Kyle Yeomans

Kyle Yeomans, Senior Undergraduate Student in Mechanical Engineering, Georgia Southern University, Statesboro, GA.

Liza Zamora

Liza Zamora, B.S. in Mechanical Engineering, First Year Graduate Student- M.S. in Applied Engineering, Georgia Southern University, Statesboro, GA.

Aniruddha Mitra

Aniruddha Mitra, PhD, PE, Associate Professor, Mechanical Engineering Department, Georgia Southern University, Statesboro, GA.

© American Society for Engineering Education, 2016